

# Thermal Conductivity Measurements of Thin Insulating Layers Deposited on High-Conducting Sheets<sup>1</sup>

M. Gustavsson<sup>2,3</sup> and L. Hålldahl<sup>4</sup>

---

The thermal conductivity of thin insulating layers and coatings deposited on high-conducting sheets has been measured using the hot disk technique. The need for this type of measurements stems mainly from the electronics industry. In many situations, the materials supporting the thin layers or films are in the shape of thin sheets—often highly conducting ceramics, metals or anisotropic composites with a high-conducting component in the plane of the sheet. The present measurement setup has some interesting advantages with possibilities to design and optimize a system for performing convenient measurements on textiles. Although apparent properties are studied in the present investigation, the need to address thermal contact problems in general engineering constructions, including interfacial layers and thermal contact resistances, is discussed here. Experiences in this field indicate that, in order to perform correct thermal analysis and design, it is necessary to treat bulk material, thermal contact resistances, and interfaces separately. This is demonstrated by the fact that there is often a difference in interface conditions when performing a measurement as compared with the situation in which a manufactured component is being used.

---

**KEY WORDS:** coatings; interfaces; layers; textiles; thermal conductivity.

## 1. INTRODUCTION

### 1.1. Thermal Conductivity and Materials Processing

Through recent developments of measurement techniques, it is now possible to perform sensitive measurements of bulk thermal transport properties,

---

<sup>1</sup> Paper presented at the Seventh Asian Thermophysical Properties Conference, August 23–28, 2004, Hefei and Huangshan, Anhui, P. R. China.

<sup>2</sup> CIT Foundation, Chalmers University of Technology, SE-412 88 Gothenburg, Sweden.

<sup>3</sup> To whom correspondence should be addressed. E-mail: Gustavsson@cit.chalmers.se

<sup>4</sup> Hot Disk AB., Salagatan 16 F, SE-753 30 Uppsala, Sweden.

and also make sensitive studies of anisotropy in the bulk thermal transport properties. Such measurements, in which the structural constitution can be correlated to the thermal transport properties, have become of interest to materials scientists working in the more applied fields of materials science.

As the thermal conductivity is strongly correlated to the structural constitution of a material [2] a sensitive measurement technique has good potential in being used as a quality control (QC) instrument. In an ongoing project at Chalmers University of Technology, together with stainless steel manufacturers, AvestaSheffield Inc. (Sweden) and Sandvik Inc. (Sweden), the hot disk technique [5, 12] is used to study thermal transport properties of well-characterized stainless steels in a single- or a duplex phase. The purpose of this study is to investigate the impact on thermal transport properties caused by different manufacturing processes, and post-processing processes such as heat treatment. Also, the structural stability is of interest. At present, significant levels and differences in thermal conductivity anisotropy (up to 10%) have been observed between cold-rolled and hot-rolled stainless steel samples of the same material [8]. Anisotropy has also been studied in other construction materials such as intermetallic TiAl alloys [13] and in wood samples [14]. For polymers that appear to be isotropic, anisotropy levels up to 30% have been observed [8].

For situations where the structure is rather complex, such as in the case of intermetallic TiAl-alloys [13], it is possible to successfully measure and correlate the thermal transport properties (including anisotropy levels) with the structural constitution.

## 1.2. Thermal Design—Industrial Needs

In thermal design and engineering today, the error sources in construction are not only associated with deviations caused by different production and processing techniques, which result in real-construction objects having thermal transport properties differing from reference data. Interfacial layers and thermal contact resistances have often a high impact in many thermal engineering situations. This is often the case for medium- and small-scale constructions involving solid–solid interfaces such as products manufactured in the electronics-, plastics-, and the ceramic-materials industries. A problem today is how to characterize and accurately take into account such influences in engineering problems.

### 1.2.1. Thermal Contact Resistance

When two solid components are mechanically clamped together, a thin imperfect solid–solid interface will appear between the two components reducing the ability of heat to flow between the components [11]. This

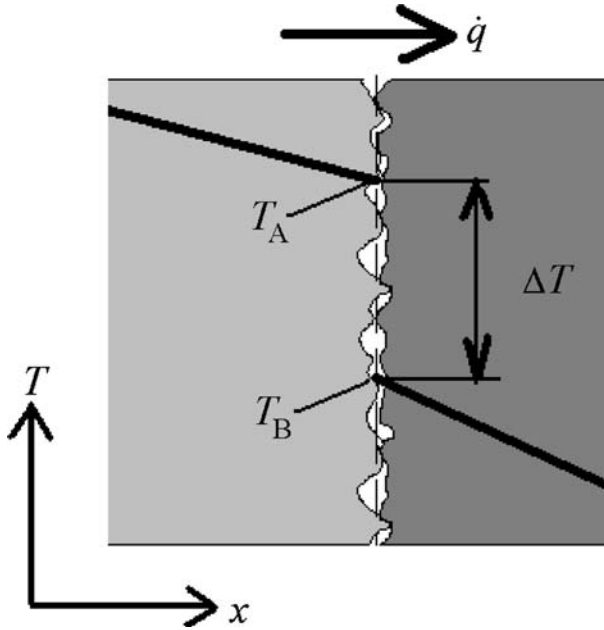


**Fig. 1.** Thermal contact resistance at a solid–solid interface causes a discrete temperature drop for a given heat flux across this layer.

thermal resistance has been found to generally behave linearly in the sense that doubling the heat flow across this layer doubles the temperature drop across this layer. If this layer is assumed to be infinitely thin—thus having a zero specific heat capacity—this interfacial layer will act as an ideal thermal contact resistance, defined by an  $R_{t,c}$ -value according to Eq. (1). Figure 1 illustrates the steady-state temperature drop across an interfacial thermal contact resistance between two different materials;

$$R_{t,c} = \frac{T_A - T_B}{\dot{q}} \quad (1)$$

In Eq. (1),  $T_A$  and  $T_B$  represents the interfacial temperatures approached from the two sides, and  $\dot{q}$  represents the heat flux.

A minor deviation from the zero specific heat assumption for this interfacial layer could be expected to have an impact on transient thermal transport analysis. However, this is seldom the case if the interface “thickness” or interface heat capacity is negligible compared with the thickness or heat capacity of the bulk surroundings. Also, if the thermal contact

resistance can be assumed to have a zero or near zero specific heat capacity, the settling time to develop a heat flow across this layer, together with an associated discrete temperature drop, can be assumed to occur instantaneously with little error. This is discussed in Ref. 15 and in Section 2.

One should, however, be careful when referring to tabular values of thermal contact resistances, as experiments are always more reliable, cf. Ref. 11. One very important issue, which has not been discussed in the thermal conductivity literature to the authors' knowledge, is the local surface roughness vs. the global surface unevenness. For hard materials like rock or ceramic materials, the local surface roughness may be a misleading indicator of the expected thermal contact resistance, as the number of contact points between two materials in contact with each other depend on the global surface unevenness—not the local surface roughness. This effect may thus result in much higher thermal contact resistances than what would be the case if the local surface roughness would define the number of contact points, which is commonly the case if one of the solids is soft and flexible. Another problem of a similar kind, which is hardly discussed in the literature, appears for coarse granular materials in contact with plane solid surfaces. At the surface, the averaged volumetric air fraction near plane surfaces is higher than the mean volumetric air fraction in the bulk granular medium. Finally, it can be noted that for materials such as polymers, which tend to relax with time, the thermal resistance across thermal contact interfaces may change with time.

For many stationary measurement techniques of thermal conductivity, such as the guarded hot plate technique, *apparent* values of the thermal conductivity are produced. With apparent values, one refers to the thermal conductivity value that is calculated from the total thermal resistance across a substrate, including thermal contact resistances at sample surfaces. The measured thermal resistance will thus generally overestimate the thermal resistance of the bulk sample, resulting in measured apparent thermal conductivity values which are lower than the bulk thermal conductivity. For stationary techniques, good reproducibility in the mounting procedure, which includes mounting pressure and surface roughness, are vital to control the impact of the surface effects. There are a couple of different but elaborate approaches to estimate and compensate for the impact of thermal contact resistances, but no accurate indicator of the difference between the measured apparent values vs. the bulk values. The reproducibility or intercomparison reproducibility between similar techniques does not imply anything on the absolute difference between bulk and apparent values—as good reproducibility in the sample preparation and mounting procedure does not necessarily keep thermal contact resistances at negligible levels. A good reproducibility in apparent values could

equally well mean a good reproducibility in reproducing thermal contact resistances at surfaces—thus reproducing the difference between measured values and true bulk properties.

### 1.2.2. Interfacial Layers

Often, adhesives or interfacial materials are introduced to enhance the thermal contact between two solid surfaces, such as thermal contact pastes. These interfacial layers are often relatively thin, and can often be analyzed in the same way as interfacial thermal contact resistances. Examples of situations in which thermal contact resistances or interfacial thermal resistance layers are critical for the application are layered electronic boards, circuits, modern Li-ion batteries, cooling of microprocessor chips, etc.

In some situations, however, one is interested to obtain the thermal conductivity of a single layer, deposited on a high-conducting background material in the shape of a sheet. This can be approached in different ways:

1. Reduce the size of the sensor and perform the measurement during short times. The pulse transient hot strip (PTHS) technique has been developed for these types of tests, cf. Refs. 1, 3, 4, 9, and 10. The advantage with this technique is that it is possible to obtain bulk properties of the deposited layer. However, the sensor needs to be manufactured by PVD-, spray-, or sputtered deposition on the sample surface.
2. Produce a composite structure, where the layer is used as an interface material between two known materials. Often, the interface material can be applied in a layered composite structure between known material sheets where it functions between each sheet in a similar manner as it would as a single interfacial layer in the real construction. Then, by studying effective anisotropic bulk values of the composite, the influence from the interfacial layer can be estimated. The advantage of this technique is that it could be the most accurate method to determine the effective impact of the layer, in both directions, if it is to be used as an interface material, cf. Ref. 8. The sample preparation needs in this case special attention, particularly if one attempts to closely reproduce the real-application condition of the layer in the composite sample.
3. Deposit a single layer on a high-conducting background. The advantage with this technique is that it is a rapid technique, where the thermal resistance across the layer or coating is measured. The disadvantage is that it is an apparent technique, which means that

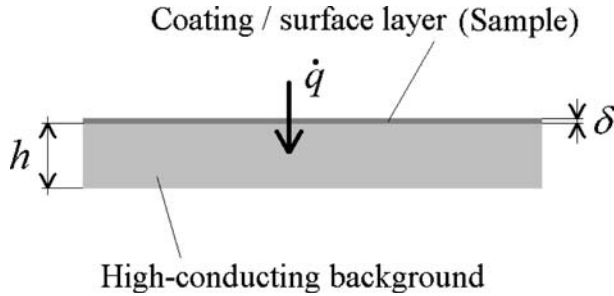


Fig. 2. Test case.

one has to consider possible influences from different thermal contact resistances in the experimental setup. Sometimes, the apparent thermal conductivity is the most relevant parameter of interest to estimate, cf. the second test case below in Section 3.

This paper demonstrates how the hot disk technique can be applied to estimate the apparent thermal conductivity of surface layers and coatings using the third approach, cf. Fig. 2. This paper also demonstrates how it is possible to measure the apparent thermal conductivity of insulating clothing and fabrics, where the properties and thickness of the background sheet can be adapted to optimize measurement parameters such as the heat flux  $\dot{q}$ , cf. Fig. 2, and the total measurement time.

## 2. EXPERIMENTAL TECHNIQUE

### 2.1. Basic Technique

Figures 3 and 4 show a hot disk sensor, and how it is applied to a sample in a basic measurement. The sensor is composed of a thin metallic strip pattern—in the shape of a bifilar spiral—encapsulated by a thin film of a polyimide on both sides.

Two pieces of the sample are required with two flat sides facing the sensor. They are clamped together—completely covering the sensor.

In the basic technique, the sensor and sample are initially allowed to settle at isothermal conditions. Then, a constant electrical power is applied to the hot disk heating element. The heat that is generated in the heating elements will then dissipate into the surrounding sample. Simultaneously, the temperature increase in the sensor heating element is recorded as a function of time. This data is then used to estimate the bulk thermal transport properties of the material.

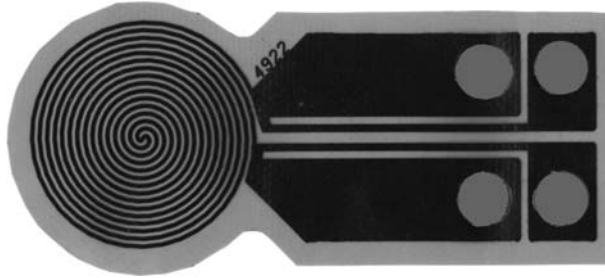


Fig. 3. Hot disk sensor.

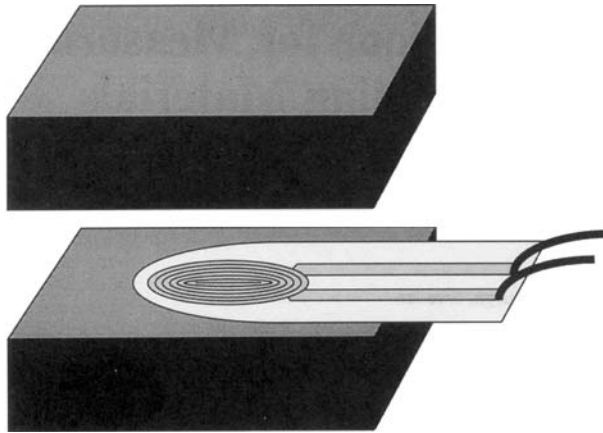


Fig. 4. Typical sample setup in a basic measurement [11].

The applied heating power causes an initial temperature increase. This initial temperature rise is mainly caused by the sensor insulation itself, but may also include interfacial thermal contact resistances. It may further include thermal resistances caused by a surface layer on the sample surface, such as a small oxide layer on the sample surface.

The model used for the analysis and curve-fitting procedure is as follows. The average temperature increase of the sensor,  $\Delta T$ , is modeled as the sum of a constant initial temperature jump  $A$  and a transient part:

$$\Delta T_i = A + \left( \frac{P_0}{\lambda_B \pi^{3/2} r} \right) D_0(\tau_i), \tag{2}$$

where  $\tau_i = \sqrt{\frac{t_i - t_{\text{corr}}}{\theta}}$  is a dimensionless time,  $t_{\text{corr}}$  is a time correction,  $t$  is the real time, and  $\theta = \frac{r^2}{a}$  is the characteristic time of the experiment

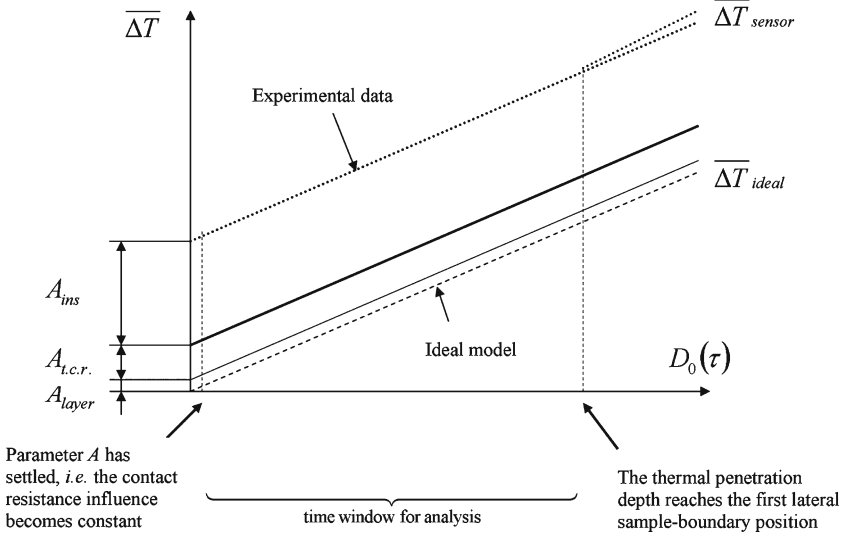


**Fig. 5.** Average temperature response as a function of  $D_0(\tau)$ , cf. Eq. (2), gives a straight-line curve fit, where the parameter  $A$  is modeled as a sum of different constant contributions to the total thermal resistance between the sensor heating element and the bulk surface, cf. Ref. 13.

[7, 8, 13, 15]. In Eq. (2),  $r$  represents the radius of the hot disk sensor and  $a$  represents the thermal diffusivity of the sample. The heating power is  $P_0$ , and the bulk thermal conductivity of the sample is  $\lambda_B$ . Index  $i$  denotes the data points, which ranges from 1 to 200.

Figure 5 displays how the model incorporates imperfect surface contact conditions in a measurement, where the average temperature increase at different locations is displayed as a function of the dimensionless time function  $D_0(\tau)$ .

The model fitted to experimental data results in a straight line—where the intercept at time zero represents the steady-state temperature difference across the interfacial layers and interfacial thermal resistances between the heating element and the bulk surface of the sample. The sensor insulation (Kapton) is  $25\ \mu\text{m}$  thick, and requires typically a settling time of the order  $\delta_{sensor}^2/a_{sensor}$ , where  $\delta_{sensor}$  represents the thickness of the insulating layer and  $a_{sensor}$  represents the thermal diffusivity of the sensor insulation layer. However, the establishment of a constant heating power is not instantaneous. Both these phenomena are treated with the use of a time correction, cf. Ref. 5, and initial points deviating from the model fitting should be omitted from the analysis.



The ideal model can be derived assuming perfect thermal contact. In Fig. 5, it represents the mean temperature increase of the bulk surface of the sample—i.e., the theoretical surface of the homogeneous bulk material.

The temperature increase at the real sample surface can be higher, which would be the case if also an additional thermal resistance, induced by an oxidation layer, would be present. At the sensor surface, the influence of the thermal contact resistance causes an even higher temperature increase. Finally, the temperature increase recorded by the sensor is significantly higher due to the thermal resistance of the sensor insulation (Kapton). The influence of these interfacial thermal resistances on the recorded temperature increase is illustrated in Fig. 5.

It can be noted that the recorded temperature increase is often much higher than the maximum temperature increase of the sample surface itself, particularly for high-conducting samples. Now, as all these interfacial influences may be summed up in the  $A$  constant, and thus be separated from the properties inside the bulk of the sample, we see that the bulk thermal conductivity may be found from the slope of the straight-line fit, and the thermal diffusivity in the best-model fitting of the  $D_0(\tau)$  function.

The model, Eq. (2), fits the experimental data quite well. For instance, with a temperature increase of the order of 1 K, the standard deviation for all curve-fitted points is of the order of  $10^{-5}$  K if the sample is homogeneous. With this sensitivity the standard deviation turns out to be of the order of 0.1% in the thermal conductivity—even if the sample is dismounted and remounted with different mounting pressures.

Unique for this technique is that the true bulk properties are determined, which makes the method appreciably more sensitive to structural changes compared with experimental methods, which are producing apparent values.

## 2.2. Thin Film Technique

The principle of the basic thin film technique is described in Ref. 7. The sensor area occupied by the double-spiral strip elements defines the heating area—normally near 50% for standard sensors, or close to 100% for thin film-sensors, where the gap between two nearly circular strips has been designed to be very small.

If using a bare sensor—a sensor without Kapton insulation—the  $A$  constant defines the temperature difference across the layer. When using a bare sensor, only electrically insulating thin films or coatings can be studied.

If a Kapton sensor is used, a reference measurement is necessary to determine the apparent thermal conductivity of the Kapton insulation. This is done by first performing a measurement of the apparent thermal

conductivity of the Kapton sensor insulation in contact with a non-covered background. The real measurement is then performed when inserting the thin film layers, giving an additional increase in the  $A$  constant. In the basic thin film technique, cf. Ref. 7, the background geometry is a standard high conducting background material, cf. Fig. 6, with smooth surfaces facing the sensor.

The present test case has one modification. The geometrical shape of the background material is different, and this setup has several interesting consequences, as demonstrated in Section 3. The background material in the present test case is a high-conducting metal sheet or slab with a well-defined thickness and smooth surfaces, cf. Fig. 6. This slab technique, cf. Ref. 6, is in a sense similar to the standard hot disk technique, but with a different  $D_0(\tau)$  function, which also depends on the thickness of the slab,  $h$ , cf. Fig. 2. With this technique, estimations are also made of the bulk properties of the slab material.

The reference measurement is generally performed using the non-covered sides of the sample so that only the Kapton influence is determined. Then, when flipping the samples so the insulating layer is in direct contact with the sensor, or inserting the thin layer between the sensor and the slab, this will result in an additional increase in the constant  $A$ . All measurements require that the two slab pieces are well thermally insulated, for instance, by Styrofoam or by a thin layer of air.

### 3. TEST CASES

In the first test case, a thin, relatively high-conducting polymer is deposited on a high-conducting sheet—and the thermal conductivity across this polymer layer is to be estimated.

The thickness of the polymer film is  $88.9\ \mu\text{m}$  (0.0035 in), and the background sheet is aluminum of 1.5 mm thickness, cf. Fig. 2. The surface of the aluminum slab sheet is rather smooth on the non-covered side, and the surface roughness of the polymer film surface is also smooth.

As the thermal contact resistance between the sensor and the surface of the coated or non-coated side is important, we expect that the reference measurement of the apparent Kapton insulation will include most of this thermal contact resistance, and that the thermal contact resistances in the two measurement cases are not too different from one another. In order to achieve a reproducible thermal contact resistance in both cases, a weight is used to give the same mounting pressure for both the reference measurement of Kapton, and the measurement with the sample. To compensate

Table I. Results of the First Test Case

Experiment No.	Kapton( $\text{m}^2 \cdot \text{K} \cdot \text{W}^{-1}$ )	Kapton + Surface coating ( $\text{m}^2 \cdot \text{K} \cdot \text{W}^{-1}$ )
1	$1.10704 \times 10^{-4}$	$1.99923 \times 10^{-4}$
2	$1.13101 \times 10^{-4}$	$2.00721 \times 10^{-4}$
3	$1.11192 \times 10^{-4}$	$2.03118 \times 10^{-4}$
Average:	$1.11666 \times 10^{-4}$	$2.01254 \times 10^{-4}$

for possible relaxation effects, the time from the mounting to the measurement is also reproduced. The measurement results are presented in Table I.

Thus, the thermal resistance caused by the  $88.9 \mu\text{m}$  ( $0.0035 \text{ in}$ ) surface coating is  $2.01254 \times 10^{-4} - 1.11666 \times 10^{-4} = 8.9588 \times 10^{-5} \text{ m}^2 \cdot \text{K} \cdot \text{W}^{-1}$ . This corresponds to an apparent thermal conductivity of  $1.01 \text{ W} \cdot \text{m}^{-1} \cdot \text{K}^{-1}$ . (Sensor used:  $3.3 \text{ mm}$  radius, assuming a 50% heating area.)

In the second test case, we wish to design an optimized test system to study apparent values of thermal conductivity of textiles and fabrics for thicknesses up to  $3 \text{ mm}$ . For textiles, it is often of interest to study apparent values.

For a particular fabric, one may be interested in studying the apparent thermal conductivity as a function of pressure—to obtain comparable properties or study the thermal conductivity as the pressure tends towards zero—or as a function of the compressed sample thickness.

There are a number of advantages when using this technique to study low-density and highly insulating clothing materials, as compared to the standard thin films technique. These are:

- Longer measurement times: For instance, using a background consisting of two smooth  $25 \text{ cm}$  (diameter)  $\times$   $3 \text{ mm}$  (thick) slab sheets of stainless steel, and using a  $60 \text{ mm}$  thin films sensor, the available probing depth in the radial direction will be  $9.5 \text{ cm}$  if the sensor is well-centered, and measurements can be performed for times as long as  $500$  or  $600 \text{ s}$ . This means that thicker fabrics can be studied, as the initial settling time to establish a constant  $A$ -value depends on  $\delta^2/a_{\text{sample}}$ , where  $\delta$  represents the measured layer thickness, cf. Fig. 2, and  $a_{\text{sample}}$  is the thermal diffusivity of the measured layer.
- Lower heating power is possible. Typically, when using a  $60 \text{ mm}$  sensor in a standard thin film measurement, a much higher power is necessary to raise the temperature of the background of the order  $1 \text{ K}$  during the shorter measurement time available. The

relatively thin background thickness in the present case keeps this power low.

- A more practical measurement setup can be designed. It is easier to control the thickness and mounting pressure between two (comparatively thin) sheets of stainless steel, than to control these for two bulk metal pieces.

The advantage of using lower heating power is that it is advantageous not to have a too large  $A$ -value in relation to the temperature increase of the background surface. A moderate increase in  $A$ , say no more than a factor 3 or 4 over the transient part, is recommended. A too high  $A$ -value in relation to the temperature increase of the transient part, say a factor of 100, will make the analysis unstable: if a constant  $A$ -value is assumed in the analysis for this situation, a 0.1% instability in the temperature drop across the layer would correspond to a 10% temperature instability in the transient temperature increase when fitting background properties,  $\lambda$ ,  $a$ , and  $\rho c_p$ . Of course, the thermal resistance is much higher for low-conducting layers such as clothing and fabrics than other higher-conducting layers, which make this technique—having the ability of working with low heating powers—an interesting option for the study of relatively thick- and highly insulating layers. In addition, the low heat capacity of clothing and fabrics (due to the low density) makes the heat input to the layers negligible as compared to the heat input to the background sheets. Table II illustrates how this system works for a couple of different samples.

In the present test case the background properties for the 3 mm thick steel sheets were reproduced to around  $\lambda = 14 \text{ W} \cdot \text{m}^{-1} \cdot \text{K}^{-1}$ ,  $a = 4.1 \text{ mm}^2 \cdot \text{s}^{-1}$ , and  $\rho c_p = 3.4 \text{ MJ} \cdot \text{m}^{-3} \cdot \text{K}^{-1}$  in all cases. A mass of 1.56 kg was used for all measurements to reproduce the mounting pressure. A number of points were omitted in the analysis, removed from the beginning of the transient—corresponding to points where the temperature difference across the cloth film had not yet settled. For a thicker sample

**Table II.** Measurement Parameters and Results of Second Test cases

Sample No.	Thickness (mm)	Power(W)	Meas. Time (S)	Th. conductivity, ( $\text{W} \cdot \text{m}^{-1} \cdot \text{K}^{-1}$ )
1 (less insulating)	0.20	3.0	40	0.0894
2 (highly insulating)	0.45	2.3	160	0.0296
3 (highly insulating)	1.00	2.0	640	0.0346

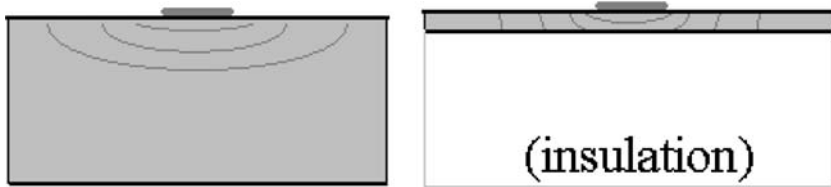


Fig. 6. Standard background sample and slab background sample.

it is necessary to have a longer measurement time so at least the second half of the transient recording can be used for the model fitting, assuming a constant  $A$ -value. The residual plot for the model fitting is a good indicator of how many points in the beginning are necessary to remove in order to obtain a linear model fitting according to Fig. 5. For these measurements the standard deviation in the model fitting was typically of the order of  $50 \mu\text{K}$ .

#### 4. CONCLUSIONS

The present technique opens up possibilities for studying the thermal conductivity of thin sheets and coatings as well as deposited layers on high-conducting slabs. The estimated thermal conductivity should be labeled as apparent—even though a compensation of the interfacial thermal contact resistance between the Kapton and the sample has been applied. If the effective impact of an interfacial material is to be determined, other methods [3, 4, 9] may prove more accurate.

The technique presented here is similar to the one used to study thin films deposited on an infinite high-conducting background. A typical feature for both these methods is that the background material must have a thermal conductivity that is at least a decade higher than that of the thin film layer.

The method has some interesting and practical implications, including a possibility to design and optimize a measurement system for conveniently studying the thermal conductivity of low-density insulating textiles with thicknesses up to around 3 mm.

#### REFERENCES

1. M. A. Chohan, *Pulse Transient Hot Strip Technique for Measurement of Thermal Properties of Non-Conducting Substances and Thin Insulating Layers on Substrates* (Ph. D. thesis, Dept. of Physics, Chalmers University of Technology, Sweden, 1987).

2. G. Grimvall, *Thermophysical Properties of Materials, Selected Topics in Solid State Physics XVIII*, E. P. Wohlfarth, ed., ISBN 0-444-86985-9 (1986).
3. S. E. Gustafsson, M. A. Chohan, K. Ahmed, and A. Maqsood, *J. Appl. Phys.* **55**:3348 (1984).
4. S. E. Gustafsson, M. A. Chohan, and M. N. Khan, *High Temp. High Press.* **17**:35 (1985).
5. S. E. Gustafsson, *Rev. Sci. Instrum.* **62**:797 (1991).
6. M. Gustavsson, E. Karawacki, and S. E. Gustafsson, *Rev. Sci. Instrum.* **65**:3856 (1994).
7. J. S. Gustavsson, M. Gustavsson, and S. E. Gustafsson, *Thermal Conductivity 24* (Technomic Publishing Co., Lancaster, PA, 1997), pp. 116–122.
8. M. Gustavsson and S. E. Gustafsson, *Thermal Conductivity 26* (DEStech Publications, Inc. Lancaster, Pennsylvania, 2001), pp. 367–377.
9. M. Gustavsson, H. Nagai, and T. Okutani, *Rev. Sci. Instrum.* **74**:4542 (2003).
10. M. Gustavsson, H. Nagai, and T. Okutani, *Int. J. Thermophys.* **26**:1803 (2005).
11. F. P. Incropera and D. P. DeWitt, *Fundamentals of Heat and Mass Transfer*, 4th Ed. (John Wiley & Sons, New York, 1996).
12. T. Log and S. E. Gustafsson, *Fire and Materials* **19**:43 (1995).
13. D. Lundström, B. Karlsson, and M. Gustavsson, *Z. Metallkd.* **92**:1203 (2001).
14. B. M. Suleiman, J. Larfeldt, B. Leckner, and M. Gustavsson, *Wood Sci. Technol.* **33**:465 (1999).
15. M. K. Gustavsson and S. E. Gustafsson, *Thermal Conductivity 27* (DEStech Publications, Inc. Lancaster, Pennsylvania, 2001), pp. 338–346.